NASA/TM—1998-206618 AIAA–98–0895

Mechanical Properties Degradation of Teflon® FEP Returned From the Hubble Space Telescope

Joyce A. Dever and Kim K. de Groh
Lewis Research Center, Cleveland, Ohio

Jacqueline A. Townsend
Goddard Space Flight Center, Greenbelt, Maryland

L. Len Wang
Unisys Federal Systems, Greenbelt, Maryland

Prepared for the
36th Aerospace Sciences Meeting & Exhibit
sponsored by the American Institute of Aeronautics and Astronautics
Reno, Nevada, January 12–15, 1998

National Aeronautics and
Space Administration

Lewis Research Center

January 1998

Acknowledgments

The authors gratefully acknowledge the contributions of Diane Kolos of NASA Goddard Space Flight Center for providing photographs of HST SM2 samples; Michael Viens of NASA Goddard Space Flight Center for performing tensile testing; Janet Barth and Shaun Thomson of NASA Goddard Space Flight Center and Teri Gregory of Jackson and Tull, Inc. for providing HST environmental exposure data; and Barry Lucas and Angela Gizelar of Nano Instruments, Inc. for providing surface hardness data.

Available from

NASA Center for Aerospace Information
800 Elkridge Landing Road
Linthicum Heights, MD 21090-2934
Price Code: A03

National Technical Information Service
5287 Port Royal Road
Springfield, VA 22100
Price Code: A03

AIAA-98-0895

MECHANICAL PROPERTIES DEGRADATION OF TEFLON® FEP RETURNED FROM THE HUBBLE SPACE TELESCOPE

Joyce A. Dever and Kim K. de Groh
National Aeronautics and Space Administration
Lewis Research Center
Cleveland, Ohio 44135

Jacqueline A. Townsend
National Aeronautics and Space Administration
Goddard Space Flight Center
Greenbelt, Maryland 20771

and

L. Len Wang
Unisys Federal Systems
National Aeronautics and Space Administration
Goddard Space Flight Center
Greenbelt, Maryland 20771

Abstract

After 6.8 years on orbit, degradation has been observed in the mechanical properties of second-surface metalized Teflon® FEP (fluorinated ethylene propylene) used on the Hubble Space Telescope (HST) on the outer surface of the multi-layer insulation (MLI) blankets and on radiator surfaces. Cracking of FEP surfaces on HST was first observed upon close examination of samples with high solar exposure retrieved during the first servicing mission (SM1) conducted 3.6 years after HST was put into orbit.[1] Astronaut observations and photographs from the second servicing mission (SM2), conducted after 6.8 years on orbit, revealed severe cracks in the FEP surfaces of the MLI on many locations around the telescope. This paper describes results of mechanical properties testing of FEP surfaces exposed for 3.6 years and 6.8 years to the space environment on HST. These tests include bend testing, tensile testing, and surface micro-hardness testing.

Introduction

The Hubble Space Telescope (HST) was designed and built to be serviced on-orbit and was deployed on April 25, 1990 in low Earth orbit (LEO) at a 595 km altitude and 28.5° attitude. To date, two servicing missions have been conducted to upgrade HST scientific capabilities. The first servicing mission (SM1) was conducted in December 1993, 3.6 years after deployment. The second servicing mission (SM2) was conducted in February 1997, 6.8 years after deployment.

The HST servicing missions provided an opportunity for on-orbit examination of second surface metalized Teflon® FEP (fluorinated ethylene propylene) on the surface of multi-layer insulation (MLI) blankets and on radiator surfaces. The HST servicing missions also provided an opportunity to retrieve materials for analysis. Minor cracking of FEP surfaces on HST was first observed upon close examination of samples with high solar exposure retrieved during SM1.[1] During SM2, astronaut observations and photographic documentation revealed severe cracks in the FEP layer of the MLI on both solar-facing and anti-solar facing surfaces of the telescope. This paper describes bend testing, tensile testing, and surface hardness measurements of HST MLI materials retrieved during SM1 and SM2.

Materials

MLI blankets are used on HST to control the temperatures on the HST Light Shield (LS), Forward Shell (FS), and Equipment Bays shown in Fig. 1. MLI blankets were also used as covers for the magnetic sensing systems (MSS) retrieved during SM1. The approximate location of the MSS covers is also indicated in Fig. 1. The MLI blankets are comprised of the following layers: The

space exposed surface is 127 μm (0.005 in.) FEP. The underside of this top FEP layer contains several hundred angstroms of vapor deposited aluminum (VDA). Underneath this aluminized FEP layer are 15 layers of 8.4 μm (0.00033 in.) double embossed polyimide, Kapton®, with VDA on both the top and bottom surfaces. The bottom layer is 25.4 μm (0.001 in.) Kapton with VDA on its top surface. The layers of the MSS MLI are held together by selective placement of acrylic transfer film adhesive and stitching. The LS, FS, and Equipment Bay MLI blankets are similarly held together with additional use of double-sided acrylic adhesive pieces to hold the layers together. During SM2 many cracks in the top layer of the LS MLI were observed. Most cracks originated at regions where there were stress concentrations from flaws, e.g. at corners, at stitch holes, or where the MLI was cut to fit around hardware.

The two largest cracks in the HST LS MLI had 127 μm (0.005 in.) FEP/VDA MLI blanket patches installed over them during the SM2 mission. A small sample of the cracked MLI was trimmed off of the LS by astronauts during patch installation and was brought back to Earth for anlaysis. The cracked material (Fig. 2(a)) had curled, with the space-exposed FEP surface facing the inside of the roll, to a diameter of 1.5 cm (as measured after retrieval), indicating a volume shrinkage gradient. As evidence of its embrittlement, this specimen broke into several pieces as a result of handling during its return to Earth. Figure 2(a) shows the specimen on the HST LS prior to removal. Figure 2(b) shows the specimen reassembled following its return to Earth. Figure 2(b) identifies pre-launch and astronaut scissor cuts, crack initiation sites (where the blanket was cut to fit around a handrail stanchion), cracks that propagated in space, and subsequent handling cracks.

Also during SM2, the cryo-vent cover (CVC) on the aft shroud of HST (Fig. 1) was removed to allow installation of a new instrument on HST. This CVC contained a thermal control coating comprised of the following components: The top space-exposed surface was 127 μm (0.005 in.) FEP. The underside of the FEP was coated with silver followed by Inconel. The FEP/silver/Inconel assembly was bonded to the CVC with an acrylic adhesive. Small x-cuts were made throughout the surface of the silvered FEP assembly to allow venting from air bubbles that were produced during bonding to the CVC. Two separate pieces of CVC silvered Teflon were removed from the CVC piece. One was removed by mechanically pulling the coating off of the CVC surface and was used for chemical analysis. The other piece was removed using acetone to dissolve the adhesive to facilitate easy removal of the silvered Teflon from the CVC. The piece that was chemically debonded was used for mechanical properties measurements. Pristine aluminized FEP was also tested and compared to the retrieved space-exposed HST materials.

Description of the HST Enviornment

The damaging effects of the HST LEO environment include solar exposure, particle radiation exposure, temperature cycling, and atomic oxygen. Potentially damaging aspects of the solar exposure environment include near ultraviolet radiation, vacuum ultraviolet radiation, and soft x-rays from solar flares. Particle radiation includes trapped electron and proton environments. Radiation absorbed within the FEP layer and/or thermal cycling may cause mechanical property changes or chemical changes within the bulk of the FEP material. Chemical changes within the bulk could also adversely affect the mechanical properties. Atomic oxygen can erode polymeric materials such as FEP through chemical reactions with gaseous oxide products.

Table 1 summarizes the LEO environmental exposures experienced by the HST-retrieved materials. Samples from the different faces of the MLI blanket used on the MSS box-shaped cover retrieved during SM1 are labeled MSS-A, MSS-B/C, MSS-D, MSS-E/F and MSS-G. Samples also include MLI from the LS and silvered Teflon from the CVC radiator surface retrieved during SM2.

Some assumptions were made in compiling the data in Table 1. First, it was assumed that all surfaces of the SM1 MSS material were subject to the same temperature range of thermal cycling. The MSS cover retrieved during SM1 was in the shape of a rectangular box cover with the surface designated as MSS-D being the top of the box and the other surfaces being the sides. Therefore, it is possible that the different orientations of these surfaces with respect to the sun may result in somewhat different thermal cycling temperature ranges. It is likely that the MSS-D surface, the top of the box, and the MSS-A surface, the most solar-facing surface of the box, most closely experienced the temperature range shown in Table 1. Also, the fluences shown in Table 1 do not take into account scattering of atomic oxygen or solar radiation off of other surfaces on the telescope. Observed degradation of the FEP surfaces will be discussed relative to the estimated exposure fluences.

Experimental Procedures

Bend Testing

Bend testing of HST exposed materials was conducted to determine differences in crack behavior for FEP materials which received different environmental exposure fluences and to determine the strain required to produce cracking.

Samples were manually bent to 180 degrees around successively smaller mandrels starting from a maximum diameter of 11.2 mm to a minimum of 0.622 mm. Samples were bent with the space-exposed FEP surface in tension to determine surface embrittlement. Some samples were bent with the back aluminum side in tension to compare embrittlement at the backside with embrittlement at the space-exposed surface. Bend testing was complete at the onset of catastrophic cracking or when the sample was bent around the minimum diameter mandrel. For mandrels between 11.2 mm and 4.47 mm the average decrease in mandrel diameter was 0.5 mm. For mandrels between 4.47 mm and 0.622 mm, the average decrease in mandrel diameter was 0.076 mm. Total number of mandrels was 53. Samples were placed around the mandrels using the least force necessary, but assuring that the samples were in good contact with the mandrel. In this way, a reasonable effort was made to produce no additional strain in the sample during the manual bending process. Samples were bent around each mandrel once, and were inspected with an optical microscope (OM). Significant changes were documented with photomicrographs.

Sample strips of approximately 20 × 5 mm were cut from pristine aluminized FEP, SM1 MSS-A, SM1 MSS-D, SM2 LS, and SM2 CVC materials. Kapton tape was adhered to the ends of each sample to provide an area that could be easily gripped during bend testing.

Tensile Testing

Tensile testing was conducted to determine degradation in tensile strength and elongation to failure for MLI and radiator surfaces exposed to the HST environment. Tensile testing was conducted using an Instron Mini Tester and strain rates of 2 to 5 in./min. Tensile specimens were "dogbone" shaped using a die manufactured in accordance with ASTM D 1822, Type L. Two to three samples each of pristine MLI, SM1 MSS-D, SM2 LS and SM2 CVC samples were tested.

Surface Micro-Hardness Testing

The surface micro-hardness of retrieved HST materials was measured to quantitatively determine the relationship between embrittlement of the materials, as evidenced by bend testing and tensile testing, and hardness. Analysis of samples was conducted by Nano Instruments using the Nano Indenter II Mechanical Properties Microprobe (MPM) with Nano Instruments' patented Continuous Stiffness Measurement technique. Hardness was measured as a function of depth up to 500 nm into the surface. Between 2 and 32 data points were taken and averaged at each depth. Samples of pristine MLI, SM1 MSS-A, SM1 MSS-B/C, SM1 MSS-D, SM1 MSS-E/F, SM1 MSS-G, SM2 LS, and SM2 CVC samples were measured.

Results and Discussion

Bend Testing

Table 2 summarizes results of the bend testing. For reference, it was verified that the FEP surface of pristine aluminized FEP did not crack when bent around the smallest diameter mandrel which produced approximately 15% strain at the FEP surface. When bend tested with the space-exposed FEP surface in tension, SM2 LS and SM2 CVC samples formed cracks and SM1 MSS samples showed worsening of pre-existing cracks. The SM2 LS material cracked differently than the SM1 MSS and SM2 CVC materials.

Each SM2 LS sample showed sudden formation of a single straight full-width crack due to bending around just one or two mandrels where there had been no previous sign of cracking. In each case, the crack formed was quite deep, leaving only a small amount of material holding the two halves of the bend-tested sample together. The SM2 LS fracture behavior is similar to that of brittle glass or ceramic materials where crack initiation is the critical stage of the fracture process. Once the crack is initiated, catastrophic fracture is inevitable, because energy absorbing processes such as plastic deformation, which would prevent crack propagation in ductile materials, do not occur. A single crack initiation site is typically observed. As shown in Table 2, cracking occurred at approximately 2 to 2.5 percent strain for SM2 LS samples. Figure 3(a) shows a photomicrograph of one of the cracks formed by bend testing the SM2 LS material. One SM2 LS bend-tested sample broke into two pieces due to handling. A scanning electron photomicrograph of the fracture surface of this sample, Figure 3(b), shows there are two distinct regions. The crack surface formed during bend-testing is the fibrous region, which accounts for approximately 80 percent of the fracture surface. The lower 20 percent of the fracture surface has long fibers of material extending from the fracture surface. These long fibers are probably the last remaining material which once held the bend-tested cracked sample together. Although it is likely that the degree of embrittlement in the SM2 LS material is a function of depth, these two distinct regions cannot be simply classified as embrittled and non-embrittled regions. The bending fracture mechanism is complicated by the fact that stress/strain will decrease after the crack is generated at the surface and continues to decrease as the crack propagates through the thickness of the specimen. Therefore, it is unlikely that the depth of the crack formed during bend testing is directly related to the depth of

embrittlement. Table 2 also shows results for two SM2 LS samples bent with the back aluminum side in tension to determine whether the back surface of the FEP Teflon was embrittled. Cracks were not produced in either of these samples when bent around the smallest mandrel which produced approximately 15 percent strain. Therefore, embrittlement is not sufficient on the backside to produce cracking at this strain level.

Results of bend testing of the SM1 MSS-A and MSS-D materials are also shown in Table 2. For these samples, hairline cracks due to handling already existed in the as-retrieved material. The data in Table 2 show the mandrel size and strain at which worsening of these existing cracks first occurred. Slight increases in length and width of existing cracks occurred as the material was bent around successively smaller mandrels. Although it was not measured, it is possible that depth of cracks also increased to some extent. However, bend-testing of these samples to the smallest mandrel did not result in deep catastrophic cracking as occurred with the SM2 LS material. Cracks formed in the SM1 MSS materials were much shallower than those formed in the SM2 LS material as evidenced by the structural integrity of the SM1 MSS bend-tested samples. Figure 4 shows an example of the jagged crack pattern as occurred in sample MSS-D.

The SM2 CVC samples showed the same type of crack behavior as the SM1 MSS material, although these samples did not contain pre-existing cracks. For these samples, cracks started as hairline cracks. Crack length and width grew gradually as samples were bent around successively smaller mandrels. As with the SM1 MSS samples, the crack path across the sample width was jagged and comprised of many cracks. All of these observations indicate that FEP from the SM1 MSS and the SM2 CVC are embrittled polymer materials, but not as brittle as the SM2 LS sample. Unlike the SM2 LS material, the SM1 MSS and SM2 CVC materials still possesses considerable fracture toughness. From these bend-testing data, one cannot conclude which material, the SM1 MSS or the SM2 CVC, is more damaged, because the SM1 MSS materials had pre-existing cracks and the CVC material did not.

The differences in the crack types and cracking mechanisms between the SM2 LS and SM2 CVC materials are likely to be related to the differences in environmental exposures received by these materials, despite the fact that they were both exposed to the space environment for 6.8 years. Because of its orientation on the HST spacecraft, the SM2 CVC material received solar exposure hours more similar to the SM1 MSS materials than the SM2 LS material as shown in Table 1. The SM2 CVC material was also subjected to thermal cycling over a shallower temperature range than the SM2 LS or SM1 MSS materials. Another important difference between the SM2 LS and SM2 CVC materials is that the LS material is aluminized FEP, which is the top surface of a free-standing MLI blanket; whereas the CVC material is a silvered FEP adhesively bonded to a plate. The effects of the space environment on the FEP surfaces may be different when the surface is constrained.

Tensile Testing

Table 3 (Reference 4) shows yield strength, ultimate tensile strength and percent elongation for each sample type. Based on loss of elongation, the ranking of samples from most damaged to least damaged was as follows: SM2 LS, SM2 CVC, and SM1 MSS-D. In general, samples showed decreased elongation to failure as a function of increasing solar exposure duration; however, there is a discrepancy in comparing the SM2 CVC and SM1 MSS results. Because the SM2 CVC and the SM1 MSS have similar levels of solar exposure, one might expect that they would be similarly degraded. However, the SM2 CVC material was significantly more degraded. As shown in Table 1, the SM2 CVC material received more electron and proton exposure than the SM1 MSS material and was subjected to substantially more thermal cycles (although over a shallower temperature range) which may account for the increased degradation observed in the SM2 CVC material as compared to the SM1 MSS material. The other differences in the SM2 CVC and SM1 MSS materials are their metal backings, silver and aluminum, respectively, and the fact that the SM2 CVC material was bonded, whereas the SM1 MSS material was the top layer of a blanket.

Surface Micro-Hardness Testing

Table 4 and Fig. 5 show the results of the surface micro-hardness measurements. The legend of Fig. 5 shows sample labels in increasing order of solar exposure. The estimated exposure environment for each sample is described in Table 1. Evaluation and comparison of hardness among SM1 samples has been previously reported by de Groh et al.[3] In general, the HST-exposed materials are harder at the surface, and hardness decreases with increasing depth into the material. According to the data in Table 4 and Fig. 5, at 500 nm depth all samples have similar hardness.

Because of the deep cracks that formed in the SM2 LS material upon bend testing, and because of the loss of bulk mechanical properties as evidenced by tensile test data, this material was expected to be significantly embrittled and, therefore, harder deeper into the material than

500 nm. Also based on the bend test and tensile test data, it was anticipated that the surface hardness would be greater for the SM2 LS material than for the SM2 CVC and SM1 MSS materials. However, this is not the case. At depths from the surface to 100nm, the SM1 materials generally show increasing hardness with increasing solar exposure; however, the SM2 LS material, which received much greater solar exposure than the SM1 materials, had surface hardness values similar to the lowest solar exposure SM1 material. Also, the SM2 CVC material which was more degraded in tensile strength and elongation than the SM1 MSS material has a surface hardness similar to the lowest solar exposure SM1 MSS material. The reasons for these discrepancies are not completely understood, but they may be related to different space environmental exposure levels or different levels of surface contamination. Such differences could significantly influence results of a surface analysis method. It is also possible that the damage necessary to cause degradation in bulk mechanical properties does not produce increased hardness in the material. It is evident that this surface analytical method is not as sensitive as tensile testing to quantitatively evaluate the significant differences in bulk embrittlement of these materials.

Summary

Solar facing second-surface aluminized FEP Teflon samples retrieved from the HST LS during SM2 were significantly compromised in their mechanical properties. Tensile strength was significantly degraded, elongation to failure was negligible, and catastrophic cracking representative of glassy fracture occurred at relatively small strain values. While the SM2 CVC materials and the SM1MSS materials also showed embrittlement and some degradation in mechanical properties, these materials still possessed considerable fracture toughness. All of these HST-exposed materials showed surface hardness values greater than that of pristine FEP, although the more degraded SM2 materials did not show greater surface hardness than the less degraded SM1 materials. This result requires further investigation. Differences in the severity of degradation among the HST-exposed materials is related to their environmental exposures including different levels of solar exposure, particle radiation exposure and temperature cycling. Further research is needed to conclusively determine the role of each environmental exposure factor in the degradation mechanisms of FEP Teflon.

References

1. Zuby, T. M., de Groh, K. K, Smith, D. C., "Degradation of FEP Thermal Control Materials Returned from the Hubble Space Telescope," NASA Technical Memorandum 104627, December 1995.
2. Milintchouk, A., Van Eesbeek, M., Levadou, F., "Soft X-ray Radiation as a Factor in the Degradation of Spacecraft Materials," Presented at the Third International Space Conference, Toronto, Canada, April 1996.
3. de Groh, K. K., Smith, D. C., "Investigation of Teflon FEP Embrittlement on Spacecraft in Low Earth Orbit," Presented at the 7th International Symposium on Materials in a Space Environment, Toulouse, France, June 1997, NASA Technical Memorandum 113153, November 1997.
4. NASA Memorandum from M. Viens to J. Townsend, "Strength Testing of HST MLI Material," dated May 1997.

TABLE 1.—ENVIRONMENTAL FLUENCES FOR HST MLI MATERIALS

Sample	Thermal cycling environment (Number of cycles; temp range)	Equivalent sun hr (albedo = earth reflected solar radiation)	X-ray fluence (J/m^2)	Trapped electron and proton fluence > 40 keV ($\#/cm^2$)	Plasma fluence, 100s eV to "a few" keV ($\#/cm^2$)	Atomic oxygen ($atoms/cm^2$)
SM1 MSS-A,	19,500 cycles −100 to + 50 °C	16,670 includes 16 percent albedo	0.5-4Å: 11.6 1-8Å: 175	electrons: 1.39×10^{13} protons: 7.96×10^{9}	electrons: 3.18×10^{19} protons: 1.11×10^{19}	7.8×10^{19}
SM1 MSS-B/C,		6,324 or 9,193 includes 72 or 33 percent albedo	0.5-4Å: 1.5 or 5.1 1-8Å: 22.1 or 77			7.8×10^{19}
SM1 MSS-D,		11,339 includes 7 percent albedo	0.5-4Å: 8.7 1-8Å: 131.8			1.56×10^{20}
SM1 MSS-E/F,		9,193 or 6,324 includes 33 or 72 percent albedo	0.5-4Å: 5.1 or 1.5 1-8Å: 77 or 22.1			7.8×10^{19}
SM1 MSS-G,		4,477 100 percent albedo	0			7.8×10^{19}
SM2 Light Shield-solar facing side (LS)	40,000 cycles −100 to +50 °C nominal; −100 to +200 °C when curled	33,638 direct 0 percent albedo	0.5-4Å: 16 1-8Å: 252.4	electrons: 2.13×10^{13} protons: 1.83×10^{10}	electrons: 4.66×10^{19} protons: 1.63×10^{19}	1.64×10^{20}
SM2 Cryo-vent cover (CVC)	40,000 cycles −80 to −15 °C	19,308 includes 33 percent albedo	0.5-4Å: 6.1 1-8Å: 96.9			

TABLE 2.—BEND TESTING OF HST SAMPLES

Sample	Surface bent in tension	Cracking occurred	Description of cracks produced/cracking process	Diameter of mandrel to produce first crack or worsening of existing cracks* (mm)	Calculated strain at first crack or first sign of worsening of existing cracks (percent)
SM2 LS-1; cut along curl direction; curl of ~1.5 cm radius	FEP	Yes	Straight/sudden, full-width	9.19	1.93
SM2 LS-3; cut against curl direction	FEP	Yes	Straight/sudden, full width	4.29	2.54
SM2 CVC-1; contains vent cut	FEP	Yes	jagged/gradual	9.19	1.63
SM2 CVC-2; typical region	FEP	Yes	jagged/gradual	7.62	1.96
SM1 MSS-A; 16,670 ESH	FEP	Yes	jagged/gradual	4.09	2.67
SM1 MSS-D; 11,339 ESH	FEP	Yes	jagged/gradual	3.56	3.05
SM2 LS-2; cut along curl direction	Al	No			Tolerant to strain >15.25
SM2 LS-4; cut against curl direction	Al	No			Tolerant to strain >15.25
Pristine MLI cut along machine direction	FEP	No			Tolerant to strain >15.25
Pristine MLI cut against machine direction	FEP	No			Tolerant to strain >15.25

*Because the SM1 MSS-A and MSS-D samples contained surface cracks due to handling upon retrieval from HST, data are for worsening of existing cracks.

TABLE 3.—TENSILE TESTING OF RETRIEVED HST MATERIALS

Sample	Yield Strength (MPa)	Ultimate Tensile Strength (Mpa)	Elongation (percent)
Pristine MLI	13.8	24.8	340
	14.3	26.5	360
	14.3	28.1	390
SM1 MSS-D	14.3	15.4	196
	14.3	16.6	116
SM2 CVC	11.0	12.1	25
	15.4	16.0	25
	N/A	11.0	15
SM2 LS	N/A	13.2	0
	N/A	2.2	0

TABLE 4.— SURFACE MICRO-HARDNESS OF RETRIEVED HST MATERIALS

Sample	Hardness at 1 to 1.5 nm	Hardness at 5 nm	Hardness at 15 nm	Hardness at 50 nm	Hardness at 100 nm	Hardness at 200 nm	Hardness at 500 nm
Pristine FEP/Al	0.27 ± 0.64 at 1 nm	0.09 ± 0.05	0.07 ± 0.01	0.07 ± 0.008	0.06 ± 0.007	0.06 ± 0.004	0.06 ± 0.002
SM1 MSS-G	0.28 ± 0.25 at 1.5 nm	0.21 ± 0.25	0.13 ± 0.03	0.09 ± 0.02	0.08 ± 0.01	0.07 ± 0.01	0.06 ± 0.004
SM1 MSS-B/C	-	-	0.26 ± 0.10	0.15 ± 0.05	0.11 ± 0.03	0.10 ± 0.01	0.08 ± 0.02
SM1 MSS-E/F	-	-	0.31 ± 0.11	0.20 ± 0.07	0.16 ± 0.03	0.11 ± 0.02	0.07 ± 0.01
SM1 MSS-D	-	-	0.34 ± 0.07	0.20 ± 0.05	0.15 ± 0.02	0.11 ± 0.02	0.07 ± 0.009
SM1 MSS-A	-	-	0.44 ± 0.14	0.26 ± 0.10	0.17 ± 0.07	0.12 ± 0.07	0.08 ± 0.05
SM2 CVC	0.35 ± 0.16 at 1 nm	0.24 ± 0.20	0.18 ± 0.10	0.18 ± 0.08	0.13 ± 0.06	0.07 ± 0.05	0.09 ± 0.001
SM2 LS	0.46 ± 0.17 at 1 nm	0.32 ± 0.26	0.14 ± 0.06	0.13 ± 0.02	0.13 ± 0.02	0.13 ± 0.04	0.10 ± 0.01

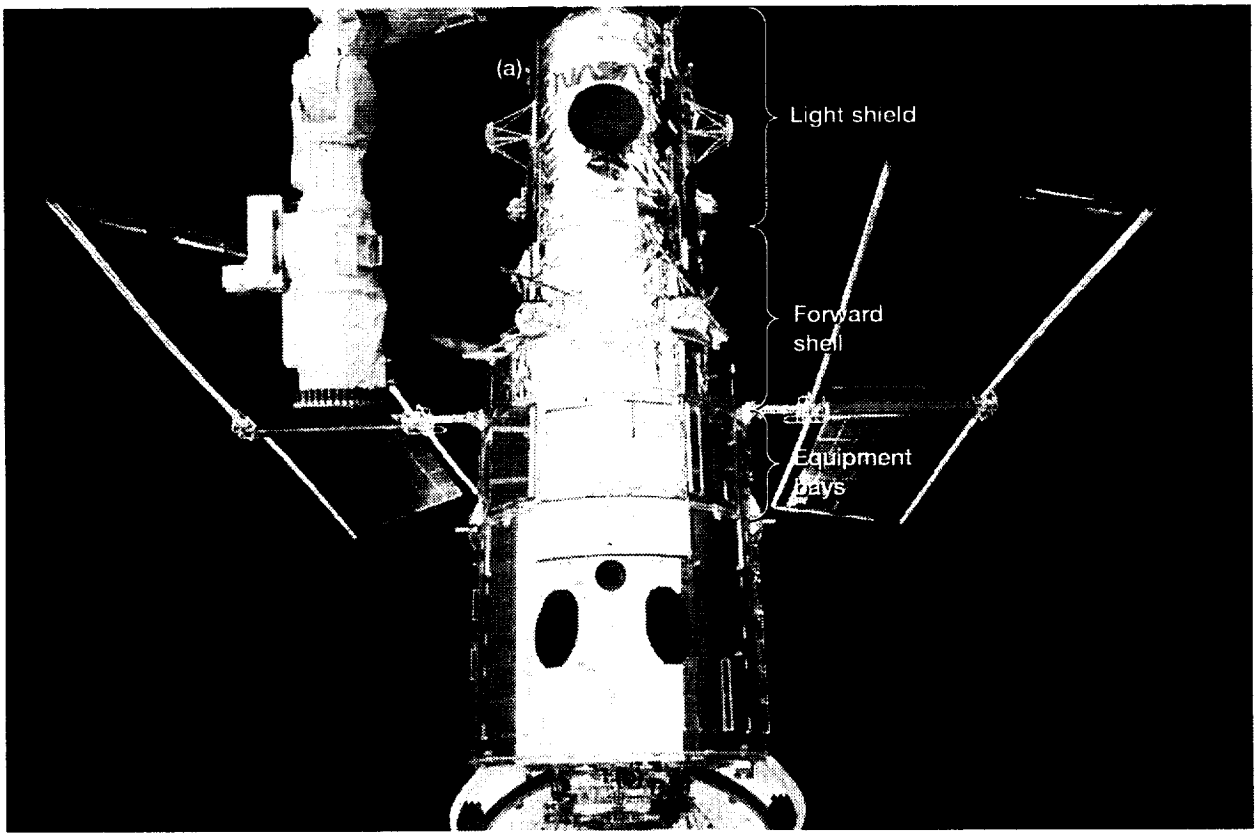

Figure 1.—Photograph of Hubble Space Telescope showing the Light Shield, Forward Shell, Equipment Bays and locations from which samples were retrieved. (a) Approximate location from which Magnetic Sensing System covers and Light Shield sample were retrieved from the opposite side of telescope. (b) Approximate location from which cryo-vent cover was retrieved.

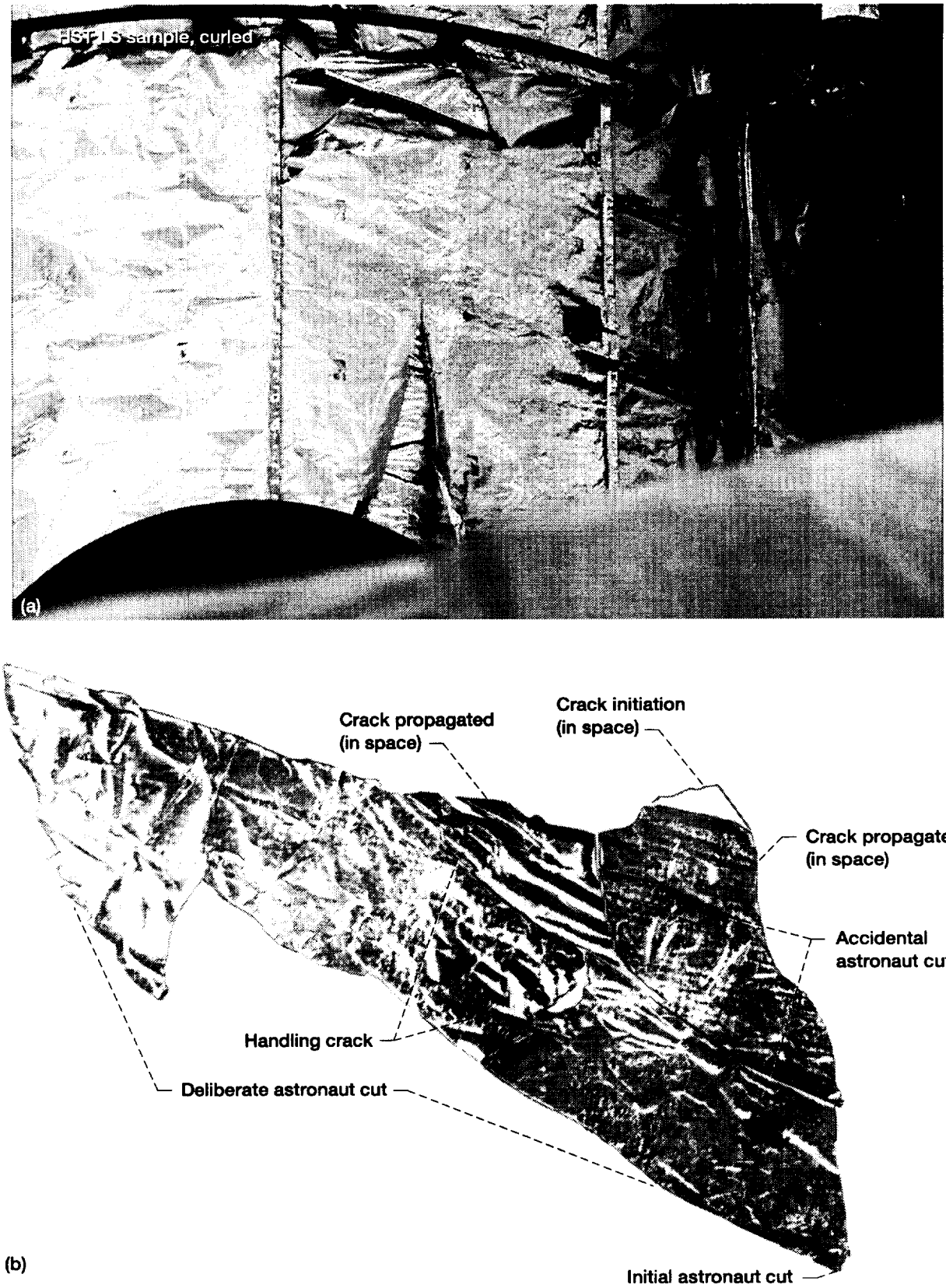

Figure 2.—HST SM2 Light Shield sample. (a) In place on the HST Light Shield prior to removal. (b) Photographs of pieces reassembled to show original configuration.

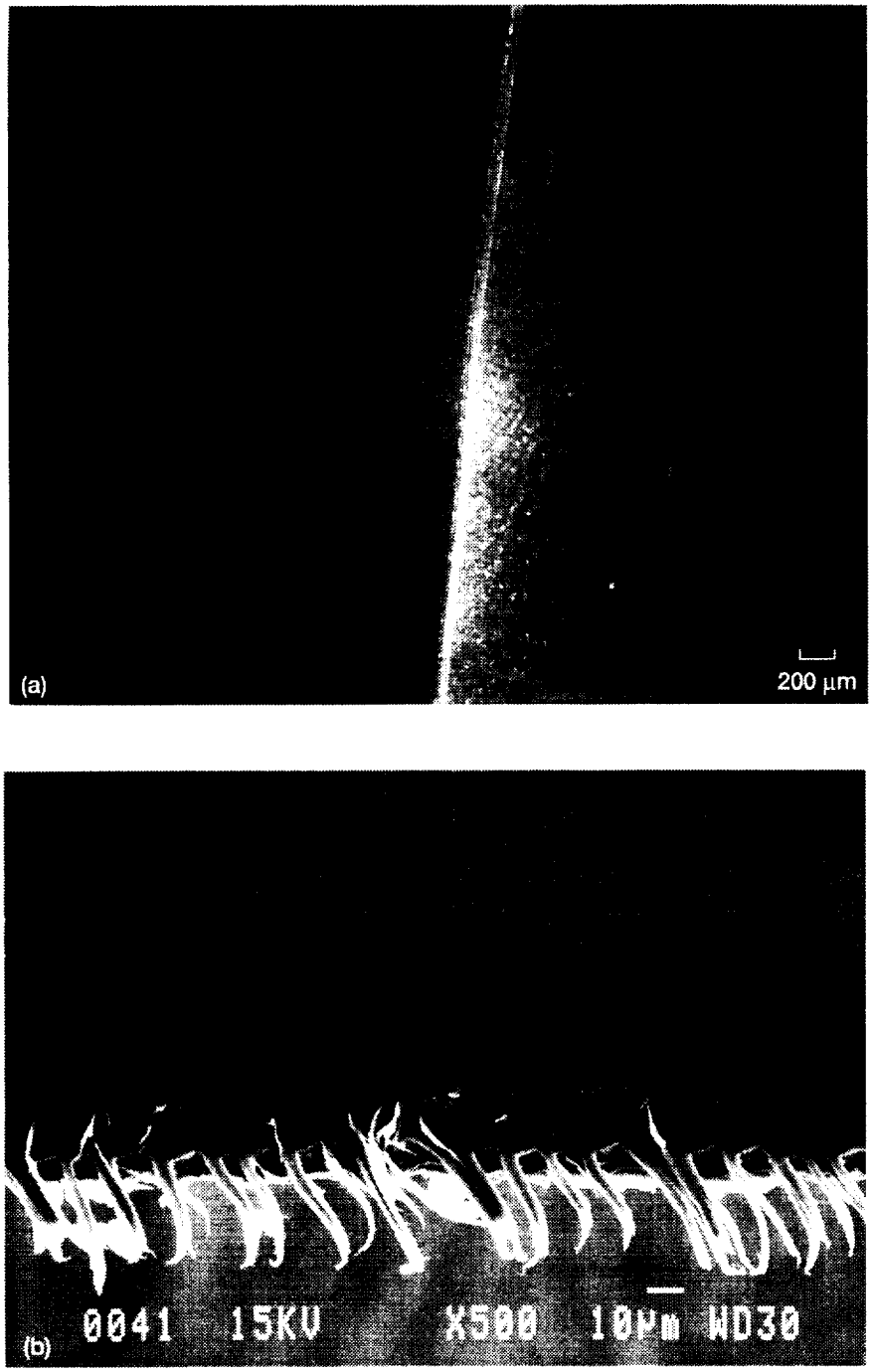

Figure 3.—Crack in HST SM2 LS sample induced by bend-testing. (a) Photomicrograph of cracked surface. (b) Scanning electron photomicrograph of cross section of crack surface.

Figure 4.—Photomicrograph of crack in HST SM1 MSS sample induced by bend-testing.

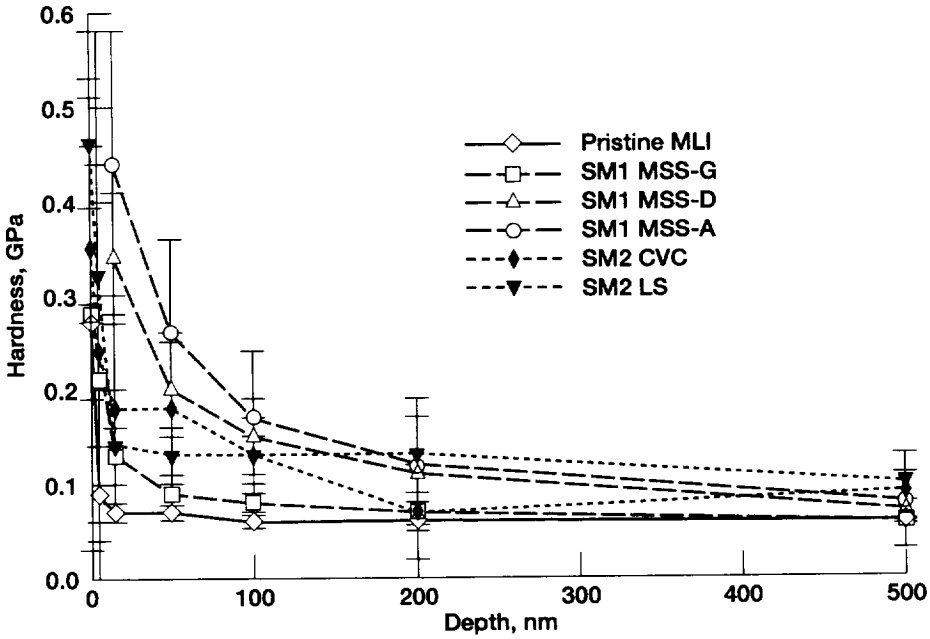

Figure 5.—Hardness of retrieved HST materials as a function of depth into the surface.

REPORT DOCUMENTATION PAGE

Form Approved
OMB No. 0704-0188

1. AGENCY USE ONLY (*Leave blank*)	2. REPORT DATE	3. REPORT TYPE AND DATES COVERED
	January 1998	Technical Memorandum

4. TITLE AND SUBTITLE

Mechanical Properties Degradation of Teflon® FEP Returned From the Hubble Space Telescope

5. FUNDING NUMBERS

WU-632-1A-1E-00

6. AUTHOR(S)

Joyce A. Dever, Kim K. de Groh, Jacqueline A. Townsend, and L. Len Wang

7. PERFORMING ORGANIZATION NAME(S) AND ADDRESS(ES)

National Aeronautics and Space Administration
Lewis Research Center
Cleveland, Ohio 44135-3191

8. PERFORMING ORGANIZATION REPORT NUMBER

E-11051

9. SPONSORING/MONITORING AGENCY NAME(S) AND ADDRESS(ES)

National Aeronautics and Space Administration
Washington, DC 20546-0001

10. SPONSORING/MONITORING AGENCY REPORT NUMBER

NASA TM—1998-206618
AIAA-98-0895

11. SUPPLEMENTARY NOTES

Prepared for the 36th Aerospace Sciences Meeting & Exhibit sponsored by the American Institute of Aeronautics and Astronautics, Reno, Nevada, January 12–15, 1998. Joyce A. Dever and Kim K. de Groh, NASA Lewis Research Center; Jacqueline A. Townsend, NASA Goddard Space Flight Center; L. Len Wang, Unisys Federal Systems, Greenbelt, Maryland 20771. Responsible person, Joyce A. Dever, organization code 5480, (216) 433–6294.

12a. DISTRIBUTION/AVAILABILITY STATEMENT

Unclassified - Unlimited
Subject Categories: 27 and 18 Distribution: Nonstandard

This publication is available from the NASA Center for AeroSpace Information, (301) 621–0390.

12b. DISTRIBUTION CODE

13. ABSTRACT (*Maximum 200 words*)

After 6.8 years on orbit, degradation has been observed in the mechanical properties of second-surface metalized Teflon® FEP (fluorinated ethylene propylene) used on the Hubble Space Telescope (HST) on the outer surface of the multi-layer insulation (MLI) blankets and on radiator surfaces. Cracking of FEP surfaces on HST was first observed upon close examination of samples with high solar exposure retrieved during the first servicing mission (SM1) conducted 3.6 years after HST was put into orbit. Astronaut observations and photographs from the second servicing mission (SM2), conducted after 6.8 years on orbit, revealed severe cracks in the FEP surfaces of the MLI on many locations around the telescope. This paper describes results of mechanical properties testing of FEP surfaces exposed for 3.6 years and 6.8 years to the space environment on HST. These tests include tensile testing, surface micro-hardness testing, and bend testing.

14. SUBJECT TERMS	15. NUMBER OF PAGES
Hubble space telescope; Teflon® FEP	17
	16. PRICE CODE: A03

17. SECURITY CLASSIFICATION OF REPORT	18. SECURITY CLASSIFICATION OF THIS PAGE	19. SECURITY CLASSIFICATION OF ABSTRACT	20. LIMITATION OF ABSTRACT
Unclassified	Unclassified	Unclassified	